Poly m-Aminophenol/ Montmorillonite Nanocomposite for Adsorption of Lead from Authentic Water Samples and Spiked River Nile Water

M. E. M. Hassouna* and M.E.M.A. Hafez

Chemistry Department, Faculty of Science, Beni-Suef University, Beni-Suef 62511, Egypt.,
mhassouna47@hotmail.com, +201223861504

Abstract— A polymer/clay nanocomposite (PCN) adsorbent was prepared from locally obtained natural raw montmorillonite clay and poly (m-aminophenol) and was used to remove lead ions from aqueous solutions. Raw clay (RC) and its sulfuric acid activated form (AAC) were also used to study the removal efficiency of lead ions. TGA, XRD, FTIR and SEM analyses were used to characterize the mineralogical compositions of (RC), (AAC) and (PCN). Batch adsorption method was applied and optimum conditions for adsorption were evaluated by changing various parameters; adsorbent dosage, contact time, temperature, pH and initial metal ion concentration. Analysis of the filtrated solutions for residual Pb^{2+} ions were conducted using ICP-MS. Langmuir, Freundlich, Tempkin, Dubinin-Radushkevich and Florry–Huggins isotherm equations have been applied to analyze the obtained experimental data. All adsorbents are best fitted with Langmuir isotherm model with affinity order PCN > RC > AAC and corresponding correlation coefficients (R^2) 0.9996, 0.9938 and 0.9904, respectively. The other isotherms affinity order were found to be for both Freundlich and Florry–Huggins AAC > PCN > RC; Tempkin PCN > AAC > RC, and for Dubinin-Radushkevich the order was PCN > RC > AAC. The maximum adsorption capacity for RC, AAC and PCN with respect to Langmuir was found to be 21.73, 24.52 and 61.81 mg/g, respectively. Adsorption kinetic models were studied and the data for PCN and AAC were fitted well by the pseudo-second-order kinetics model with $R^2 = 0.9999$, while RC was fitted well by pseudo-first-order and liquid film diffusion kinetics model. The spontaneity of the adsorption process for each type of clay was proven by the negative value of ΔG^o, the other thermodynamic parameters ΔH^o and ΔS^o were also studied for further interpretation. The method was applied on real surface water samples obtained directly from the River Nile and spiked with lead ions. The three adsorbents proved efficient in adsorbing lead ions.

Keywords— Polymer/clay nanocomposite, XRD, TGA, FTIR, montmorillonite, lead, adsorption, removal, acid activated, water treatment, isotherms, kinetics.

INTRODUCTION

Enhanced industrial activity during recent decades has led to the discharge of unprecedented volumes of wastewater, which is a serious cause of environmental degradation.If these volumes of wastewaters were discharged directly into natural waters, it will constitute a great risk for the aquatic ecosystem. The removal of toxic heavy metals or decreasing their concentrations to the permitted levels before discharge in theecosystem has becoming more important with the increase in industrial activities. The discharge of untreated industrial wastewater in streams, rivers and lakes, has been responsible for several types of health problems in all living systems[1-6].Within the European community, the 13 elements of highest concern are As, Cd, Co, Cr, Cu, Hg, Mn, Ni, Pb, Sn,and Ti, the emissions of which are regulated in waste systems. Some of these elements are actually necessary for humans inminute amounts (Co, Cu, Cr, Ni) while others are carcinogenic or toxic, affecting, among others, the central nervous system (Hg,Pb, As), the kidneys or liver (Hg, Pb, Cd, Cu) or skin, bones, or teeth (Ni, Cd, Cu, Cr) [7-9].

They have non-biodegradable nature and the risk of entry into the food chain or into the water supply [10] that leads to bioaccumulation in living organisms causing health problems in animals, plants, and human beings. One of such heavy metals of concern is lead. Lead is a highly toxic heavy metal even at a trace level, it was known to be harmful to human health if ingested or inhaled.(WHO). Complain about exposure to lead in the womb and during childhood that reduces intelligence quotient (IQ) [11]. Lead in the body can damage the brain, kidneys, nervous system, and red blood cells. Children, infants, pregnant women, and their unborn children are especially vulnerable to lead [11-13]. In children, lead has been associated with the impaired mental and physical development as well as hearing problems. The harmful effects of lead in the body can be subtle and may occur without any obvious signs of lead poisoning. Lead also cause mental retardations, reduces haemoglobin production necessary for oxygen transport and it interferes with normal cellular metabolism [14-16]. The Environmental Protection Agency (EPA) has set a cumulative blood lead level to remain below 10 µg/dL. EPA and WHO limit in drinking water is 15 µg/l.

Lead is a common metal found throughout the environment in the air, lead-based paint, soil, household dust, canned food, porcelain, production of petroleum products, batteries, accumulators, paints, printed circuit boards, pewter, certain types of pottery and mining activities. Lead is also present in plumbing fixtures [11-13, 17-19].Plumbing for several hours or more, lead may dissolve into the water. Also, the dismantling of waste electrical and electronic equipment (WEEE) industry yields high Pb margins. The numerous sources of lead in the environment make it one of the commonly found metal ions in water and wastewater solutions.

Various methods for heavy metals removal have been used include chemical precipitation, membrane filtration, ion exchange, reverse osmosis, electrochemical treatment, and evaporative recovery [20]. The application of such processes is often limited because of technical or economic constraints. Besides these techniques, adsorption is the most attractive option. The prevalence of adsorption separation [21-33] in the environmental chemistry remains an aesthetic attention owing to its low initial cost, effectiveness, local availability, sustainability, simplicity of design, ease of operation, sensitivity to toxic substances and complete removal of pollutants even from dilute solutions. In addition, owing to the reversible nature of most adsorption processes, the adsorbents can be regenerated by suitable desorption processes for multiple use [34, 35], and many desorption processes are of low maintenance cost, high efficiency, and ease of operation.

The high cost of activated carbon has motivated scientists towards the search for new low cost adsorption means. Clays are natural environment friendly materials with high specific surface area showed a large participation in waste water treatment. A large number of clays have been utilized as adsorbents: siderite [36], clinoptilolite [37], natural and conditioned clinoptilolites [38], Tunisian smectitic [39], bentonite [40], zeolite [41], clay minerals [42], synthetic Goethite [43] and bio-inspired polydopamine coated natural zeolites [44]. Recently, nanoparticles have been extensively used for the ease of modifying their surface functionality and their high surface area to volume ratio for increased adsorption capacity and efficiency [2, 22, 45].

Numerous biosorption matrials have been used for the removal of lead ions such as: ground nut shells [1], palm fiber [14], husk and modified rice husk [15], waste tire rubber ash [18], biomass adsorbents [20, 26], chitosan [46], chitosan-enhanced membrane filtration [47]. Also some fungi like Asperigillus niger [27] have the ability to accumulate heavy metals from the toxic environment.

In the last few years, polymer/clay nanocomposites have received a great deal of attention as sorbents for the toxic heavy metals in the wastewater streams. Nanocomposites often exhibit physical and chemical properties that are dramatically different from conventional microcomposites. The increasing attention devoted to polymer/clay nanocomposites arises from the fact that presence of relatively low amount of clay mineral in the polymerization procedure gives the possibility to modify drastically some of its chemical and physical properties for the resultant polymer/clay nanocomposite.

In the present study, natural raw clay RC having low or even no cost, obtained from Gebel Qarara Beni-Suef city, Egypt, was used in the design of PCN. The RC and its acid activation form by sulfuric acid were also performed in order to compare its removal efficiency in adsorbing lead ions. Batch experiments were conducted to investigate the adsorption affinity, kinetics and equilibrium isotherms of the prepared composite towards Pb^{2+} ions in aqueous solution. After each experiment, aliquots of the treated samples were separated by filtration, followed by analysis of the filtrate for residual Pb^{2+} ions using ICP-MS.

Materials and Method

Adsorbent Materials

RC: Natural raw clay mineral was obtained from Gebel Qarara, Beni-suef, Egypt. The clay was dried at room conditions for two weeks then crushed by Jaw crusher, grinded in a ball mill and sieved to pass completely from 125 μm sieve. The grinded clay was purified by washing several times with distilled water (>18 MΩ) until the supernatant became clear from any deterioration, filtered and dried at 80°C over night. Finally the RC was grinded in a ball mill to nano-size and stored in a desiccator for further study.

AAC: Fifty grams of the purified RC mineral were activated by refluxing with 1000 mL 1M H_2SO_4 at 80 °C for 2 h with vigorous and continuous stirring. The precipitate was washed twice with deionized water by decantation. The activated clay was filtrated and washed with deionized water more than five times until the washings were free from SO_4^{2-} tested by lead acetate solution 0.01 M. The precipitate was dried under vacuum at 90 °C for three hours. Finally the product was grinded and stored in the desiccator.

PCN: Poly m-aminophenol/clay nanocomposite has been synthesized using a pseudo dispersion oxidative polymerization of m-aminophenol (mAP) in aqueous HCl medium using ammonium persulfate (APS) as oxidant. At first, 50 g of the purified RC mineral was added to 350 mL deionized water under vigorous stirring to form a suspension. The clay suspension was ultrasonicated for 30 min to improve dispersion. A solution of 22.917 g mAP (0.21 mol.) in 350 mL 1 M HCl was poured into the suspension; and sonication was continued to one hour. Then, 95.844 g APS (0.42 mol.) dissolved in a minimum volume of water was poured once which the drop-wise addition was avoided as it gave low yield. A thermostat was inserted to measure the temperature change during polymerization and the reaction mixture was sonicated continuously in an ice–bath for 10 h at 10–20 ^{o}C. A dark brown precipitate of PmAP/clay nanocomposites was filtered and washed 4–5 times with 4 M HCl in order to remove unreacted monomers or oligomers. The precipitate was further washed with deionized water for several times till the pH of the washings becomes neutral. The resulting product was finally dried at 60–70 ^{o}C in a vacuum oven for about 12 h.

Batch adsorption experiments for lead were studied at room temperature. After each Batch experiment, aliquots of the treated samples were separated by filtration, followed by analysis for residual Pb^{2+} ions using ICP-MS.

Determination of the optimum adsorbent amount:

Initial metal concentrations of 120, 57.14 and 400 mg Pb^{2+}/L at pH 5.25 were used to optimize the adsorbent dosage for RC, AAC and PCN, respectively. The amounts of adsorbent used for RC and AAC were (0.05, 0.1, 0.15, 0.2, 0.3, 0.4 and 0.5 g), these dosages were added to 35 mL of the heavy metal solution in a 40 mL vial. But for PCN use (0.06, 0.08, 0.1, 0.12, 0.14, 0.16 and 0.18 g), these dosages were added to 10 mL of the heavy metal solution in a 20 mL vial. Vigorous stirring was applied for one hour contact time at room temperature 25 ^{o}C.

Determination of the optimum agitation contact time:

The agitation contact time was investigated for 15, 30, 45, 60, 90, 120, 150 and 180 min. The reaction was done at room temperature 25 ^{o}C with optimized adsorbent dosage 0.2, 0.15 and 0.1 g for RC, AAC and PCN, respectively.

Determination of the effect of temperature:

Water bath equipped with a temperature controller was used to examine the effect of temperature on the adsorption process. Different temperatures 25, 30, 40, 50, 60 and 70 ^{o}C were investigated for each type of clay.

2.3.4. Determination of the optimum pH value:

At room temperature 25 ^{o}C, the initial pH values of solution were adjusted by adding nitric acid or sodium hydroxide at 2, 3, 3.5, 4, 4.5, 5, 6, and 7. Buffering wasn't used in the experiments due to unknown effects on the adsorption process.

Determination of the optimum metal concentrations

Different Initial metal concentrations ranged from100 to700 mg Pb^{2+}/L were prepared. The reaction solutions had pH 5.25 and were allowed to proceed at room temperature 25 ^{o}C.

Real sample treatment

Surface water samples were obtained from the River Nile and their pH was adjusted to 5.5. The samples were spiked with lead ions to prepare 200 mg Pb^{2+}/L. A 0.5 g of each adsorbent was added to 100 mL of the 200 mg Pb^{2+}/L solution in order to study the removal efficiency. The reaction mixture was allowed to proceed at room temperature for 3 hours agitation time followed by analysis of the filtrate for residual Pb^{2+} ions using ICP-MS.
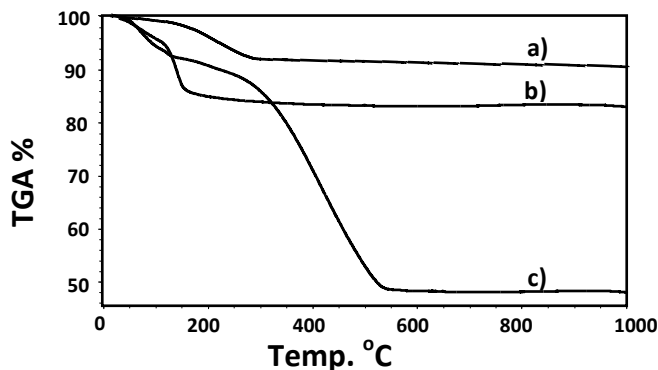
Results and Discussions

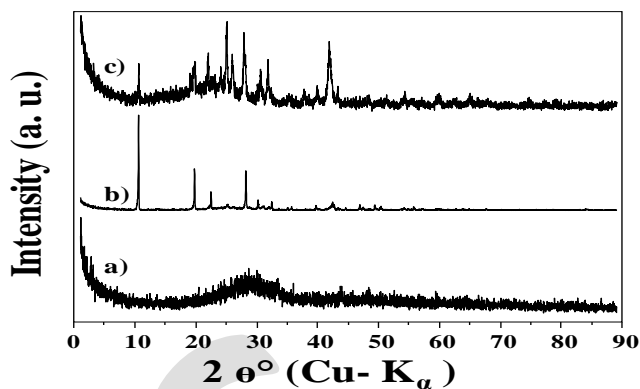**Fig.1.** Thermal gravimetric analysis for: a) RC, b) AAC and c) PCN.

Fig.2. X-ray diffractograms of: a) RC, b) AAC and c) PCN.

The changes in weight of the investigated clay samples were studied by thermal gravimetric analysis as shown in figure (1). It is clear that RC and its activated form reveal three weight loss steps. The first one is slow at the temperature range 30 to 150 °C corresponding to the liberation of the mechanically held water, with a weight loss of about 2 %. The second stage lies between 150 and 300 °C which is very fast and characterizes the dehydration of iron bearing minerals, the weight loss amounts to about 5.5 %. The last weight loss occurs at the temperature range 300 to 1000 ºC which confirms the evolution of the lattice hydroxyl groups of the clays as well as the dissociation of dolomite, with a weight loss of about 1.5 %. Four weight losses were recorded for PCN. The first is slow with weight loss of 8% at temperature range 30 to 150 °C, is attributed to the liberation of the mechanically held water in the clay minerals and the release of bound water molecules present in the polymer sample. The second weight loss of 6% at temperature range 150 to 300 °C is attributed to the dehydration of iron bearing minerals and trace decomposition at 300 °C, this is due to the release of some decomposition products, which might be O_2 and H_2O molecules [48, 49]. The third weight loss of 36.2% at temperature range 300 to 545 °C which is attributed to the total decomposition of poly (m-aminophenol) in the form of CO_2, NO_x and H_2O gases. The last weight loss of 1.8% from 545 to 1000 ºC which confirms the evolution of the lattice hydroxyl groups of the clays.

Identification of clay minerals by (XRD) is based on the determination of the lattice spacing d (Å) which is the distance between the two successive lattice planes. Bragg's equation is used to calculate the lattice spacing as follows [50]:

$$n\lambda = 2d(hkl)\sin\theta$$

where hkl is the index of the reflecting plane, λ is the wave length of radiation, n is an integer number usually used equals one, d is lattice spacing and θ is the angle of incidence. The XRD patterns of the studied clay samples are shown in figure (2). ASTM cards for clay and non-clay minerals were used in the identification of the mineral composition of the studied samples. The results revealed that the investigated RC and PCN contain some quartz, montmorillonite, illite, kaolinite, and dolomite. For AAC, the kaolinite is converted to gypsum which is the main cause for decreasing its removal efficiency which is less than that of RC. On the other hand, montmorillonite represents the major clay mineral content of the studied samples.
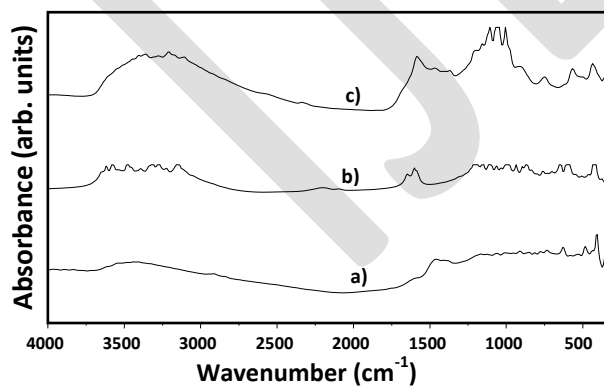

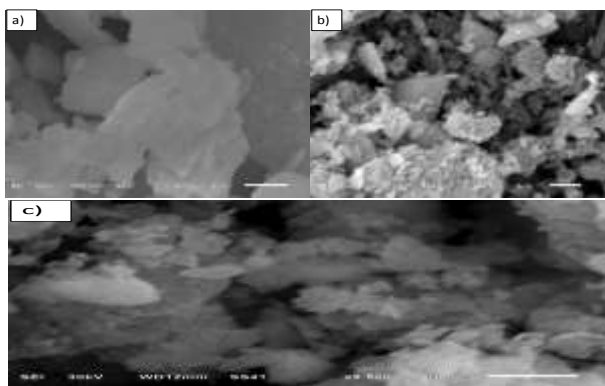**Fig.3.** FT-IR spectra of: a) RC, b) AAC and c) PCN.

Fig.4. SEM images of: a) RC, b) AAC and c) PCN.

The characteristic vibrational bands obtained from FTIR spectra of PCN figure (3) proved the successful preparation of the poly meta-aminophenol [48, 49, 51]. A broad band appears in the region 3690–1833 cm^{-1} which is due to the stretching of aromatic C–H, hydrogen bonded –OH, and –NH– groups. The –OH group is hydrogen bonded with the nearest nitrogen of –NH group

9

present in the polymer chain. So –OH absorption band appears at about 3425 cm^{-1} as a broad peak. There is a band at 1050 cm^{-1} due to bending vibration of aromatic C–O–H group present in the polymer. The band at 1236 cm^{-1} is close to C–O stretching band at 1265 cm^{-1} as an overlapping broad band. Due to the band at 1050 cm^{-1} and a very weak band at 1236 cm^{-1}, it is expected that very little C–O–C linkage was formed in the polymer. That means most of the –OH groups remain free after polymerization.

As shown in figure (4), the morphological structure of RC figure (4a) appears in micrometer scale with uniform arrangement of the clay silicate layers stacked together in form of agglomerates. This formation was disappeared in PCN SEM micrograph figure (4c); this was attributed to the single nano polymer chains that are intercalated between unaltered silicate layers. The single clay layer with nanometer width spreads on the polymer matrix. The SEM image of AAC figure (4b) show different particle morphology than RC. The large flat layers of RC change to smaller layers and fragmented pieces caused by acid treatment effect [52, 53].

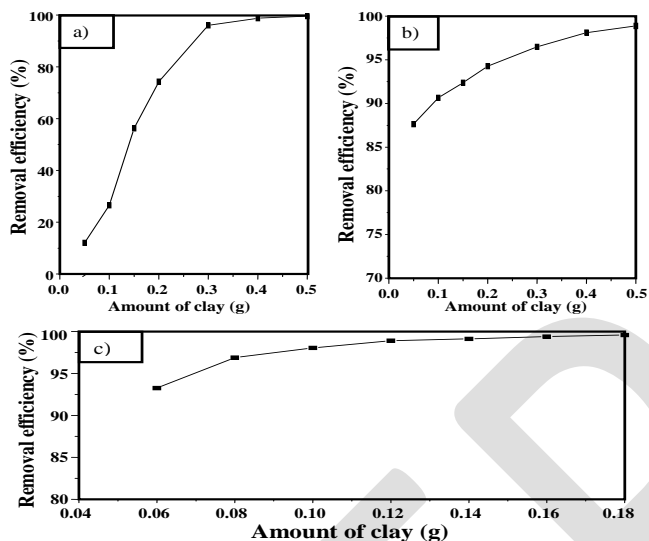## Effect of adsorbent dosage and contact time on the adsorption process

Fig.5. Effect of the adsorbent dosage on the adsorption

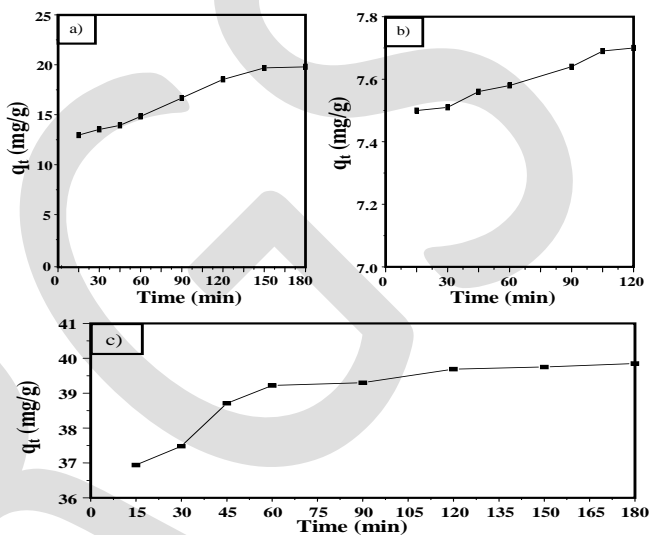of Pb^{2+} ions: a) RC, b) AAC and c) PCN.

Fig.6. Effect of the contact time on the adsorption of Pb^{2+}

ions: a) RC, b) AAC and c) PCN.

As expected, the removal efficiency is increased with increasing the adsorbent dose for a given initial metal concentration. This is due to the increase of adsorbent dose that is proportional to the increase of number of adsorption sites and surface area which is attributed to the binding of metal ions onto the surface functional groups present on the adsorbent surface. The effect of RC, AAC and PCN dose on the percentage removal of Pb^{2+} ions was shown in figure (5). From the figure it can be observed that the percentage removal of lead ions was increased from 12.02% to 99.56% when the adsorbent dose was increased from 0.05 g to 0.5 g in case of RC. For AAC, the percentage of lead removal was increased from 87.63% to 98.88% when the adsorbent dose was increased from 0.05 g to 0.5 g. The percentage of lead removal began very high 93.26% for PCN compared with RC and AAC till reached 99.58% when the adsorbent dose was increased from 0.06 g to 0.18 g. By the end of adsorbent dosage study we consider the optimum dosage was 0.2, 0.15 and 0.1 g that achieved removal efficiency 71.44%, 92.36% and 98.06% for RC, AAC and PCN, respectively.

The effect of contact time on adsorption of Pb^{2+} ions is shown in figure (6). The adsorption of lead ions was increased by increasing the contact time. The adsorption process was faster in the first 60 min for both RC and PCN; and then became more slowly until they reached equilibrium at 150 and 120 min.; and achieving adsorption capacity of 18.54 and 39.7 mg/g, respectively. The adsorption rate in case of AAC began slowly until it reached equilibrium at 120 min. achieving adsorption capacity of 7.7 mg/g. It was found that; the adsorption of Pb^{2+} ions using PCN reached equilibrium within 120 min with removal capacity 39.7 mg/g indicating the strong ability of this adsorbent to abstract Pb^{2+} ions from aqueous solutions. The higher amount of adsorption by PCN could be rationalized in terms of increasing both the active sites and the surface area according to the presence of the polymer chains.

Adsorption kinetics

The relationship between adsorption capacity and adsorption time represented in figure (6) is used to describe the adsorption kinetics. The adsorption kinetics is one of the important characteristics defining the efficiency of an adsorbent. It describes the solute uptake rate which evidently controls the diffusion process and the residence time of adsorbate uptake at the solid−solution interface. In order to analyze the adsorption mechanism of Pb^{2+} ions onto the different types of clay; Lagergren pseudo-first-order and pseudo-second-order [54-57] adsorption kinetics models were applied to fit the obtained experimental data and to investigate the adsorption properties of each adsorbent.

The pseudo-first-order kinetic model of the Lagergren is one of the most widely used for the adsorption of a solute from liquid solutions and can be expressed by:

$$\frac{dq_t}{dt} = k_1(q_e - q_t) \quad \text{which can be expressed in linear form as} \quad \ln(q_e - q_t) = \ln q_e - k_1 t$$

The chemisorption pseudo-second-order kinetic model is represented by:

$$\frac{dq_t}{dt} = k_2(q_e - q_t)^2 \quad \text{which can be expressed in linear form as} \quad \frac{t}{q_t} = \frac{1}{k_2 q_e^2} + \frac{t}{q_e}$$

where k_1 and k_2 are the adsorption rate constants of first-order and second-order kinetic models (1/min and g/mg min), respectively; q_t and q_e (mg/g), are the respective adsorption capacity of the metal ion at a time t and at equilibrium, respectively. The slopes and the intercepts of each linear plot in figure (7) are used to calculate the adsorption rate constants (k_1 and k_2) and the amount of adsorption at equilibrium (q_e). The calculated kinetics parameters for adsorption of Pb^{2+} ions onto the different types of clay are listed in Table 1.
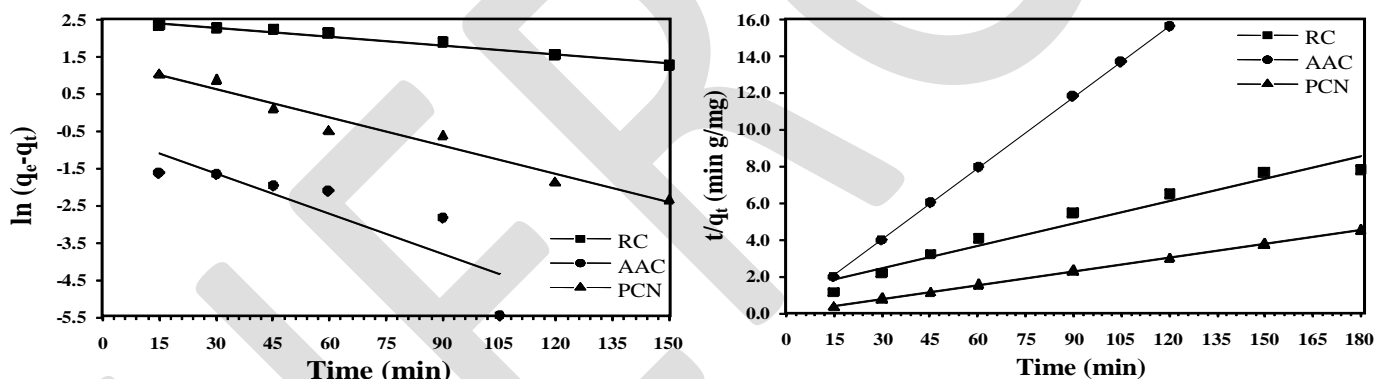

Fig.7. The first and second-order kinetic model for the adsorption process.

Table 1. Kinetic model parameters for the adsorption of Pb^{2+} ions onto RC, AAC and the PCN:

Kinetic models	Parameters	RC	AAC	PCN
Pseudo first-order	K_1 (min^{-1})	0.0082	0.0360	0.0255
	q_e cal. (mg/g)	12.724	0.5696	4.1055
	S.D.	0.0714	0.8452	0.2521
	R^2	0.9746	0.7326	0.9677
Pseudo second-order	K_2 (g/mg min)	0.0014	0.1466	0.0141
	q_e cal. (mg/g)	24.504	7.7393	40.225
	S.D.	0.5463	0.0429	0.0073
	R^2	0.9582	0.9999	0.9999
Experimental	q_e Exp. (mg/g)	23.2	7.7	39.851

Referring to Table 1, the correlation coefficients (square of regression (R^2) values close or equal to 1) is an expression for the conformity between the experimental data and the model. A relatively high R^2 value for a model indicates that this model is successfully describing the kinetics of Pb^{2+} ions adsorption. The favorability of RC to follow Lagergren kinetic model is found to

be high as confirmed by the highest value of the square regression (R^2) 0.9746. The adsorption of Pb^{2+} ions by each of AAC and PCN didn't fit well the first-order Lagergren kinetic model. The second-order kinetic model is fitted well in case of the adsorption of Pb^{2+} ions on AAC and PCN (square of regression 0.9999 for both) indicating that the adsorption process might be a chemical adsorption (chemisorption) involving valence forces through sharing or exchange electrons between the sorbent and adsorbate. In chemical adsorption, it is assumed that the adsorption capacity is proportional to the number of active sites occupied on the adsorbent surface. Fitted equilibrium capacities (q_e, cal) are in close agreement with those observed (q_e, exp) experimentally as clearly shown in Table 1. The experimental data so far revealed that PCN is an efficient adsorbent for the removal of lead ions from aqueous solutions where the adsorption capacity reaches 39.85 mg/g within 120 min.

The adsorption data may also, be described by some adsorption diffusion models which are always constructed on the basis of three consecutive steps: (1) film diffusion (i.e., diffusion across the liquid film surrounding the adsorbent particles); (2) intraparticle diffusion (i.e., diffusion in the liquid contained in the pores and/or along the pore walls); and (3) mass action (i.e., physical adsorption and desorption between the adsorbate and active sites). Since the adsorption step is very rapid, it is assumed that it doesn't influence the overall kinetics. The overall rate of adsorption process will be controlled by either surface diffusion or intraparticle diffusion. The intraparticle diffusion model[58, 59] assumes that the metal ions are transported from the solution through an interface between the solution and the adsorbent which called film diffusion, followed by a rate-limiting intraparticle diffusion step which bring them into the pores of the particles in the adsorbent.

Isotherm Analysis

For analyzing the experimental data, adsorption isotherm models were used to determine the homogeneous and heterogeneous characteristics. To evaluate the adsorption isotherm, two equilibrium isotherms were studied: A) Langmuir & B) Freundlich. Analysis of isotherms was used to describe the experimental adsorption data, and then best results can be obtained when correlation coefficients (R^2) come close to 1, Table 2. High values of R^2 (close or equal to 1) indicate the conformity among experimental data with the isotherm model.

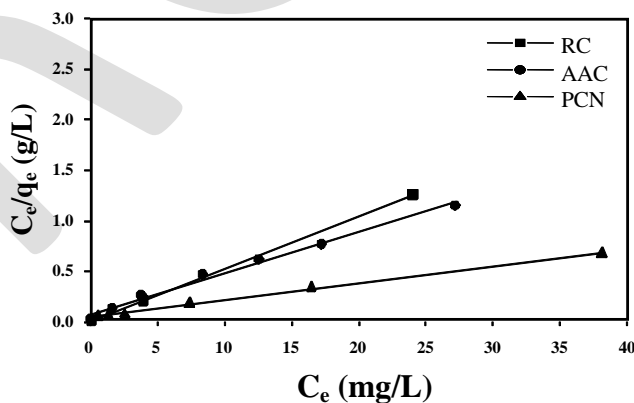| Equilibrium models	Parameters	RC	AAC	PCN
Langmuir	Q_m (mg/g)	21.734	24.581	61.805
	K_L (L/mg)	-4.5064	0.5913	0.2816
	S.D.	0.2566	0.0427	0.0124
	R^2	0.9938	0.9904	0.9996
Freundlich	K_F (mg/g)(L/mg)$^{1/n}$	18.219	13.007	16.947
	n_F	25.667	5.8323	3.0467
	S.D.	0.0548	0.0631	0.2486
	R^2	0.8167	0.9661	0.8769

Table 2. Equilibrium isotherm model parameters for the adsorption of Pb^{2+} ions onto RC, AAC and PCN

Fig.8. The Langmuir isotherm model for the adsorption process

Langmuir adsorption isotherm [60] describes quantitatively the formation of a monolayer adsorbate on the outer surface of the adsorbent [61] and after that no further adsorption takes place [62]. The Langmuir isotherm is valid for monolayer adsorption onto a surface containing a finite number of identical sites. Langmuir model assumes that adsorption forces are similar to the forces in chemical interactions, uniform energies of adsorption onto the surface and no transmigration of adsorbate in the plane of the surface. Based upon these assumptions, Langmuir represented the following equation:

$$q_e = \frac{Q_m K_L C_e}{1 + K_L C_e}$$ which can be expressed in linear form as $$\frac{C_e}{q_e} = \frac{C_e}{Q_m} + \frac{1}{Q_m K_L}$$

where C_e is the concentration of Pb^{2+} ions at equilibrium (mg/L), q_e is the adsorption capacity at equilibrium (mg/g), Q_m is the maximum adsorption capacity at monolayer coverage (mg/g) and K_L is the intensity of adsorption (L/mg). Figure (8), illustrates a plot of C_e/q_e versus C_e, enabling the calculation of Langmuir constants from the intercept and slope of the linear plot.

Langmuir isotherm model assumes the mechanism of the adsorption process as a monolayer adsorption on completely homogeneous surfaces where interactions between adsorbed molecules are negligible [63]. This empirical model assumes that the adsorbed layer is one molecule in thickness, with adsorption can only occur at a fixed number of definite identical and equivalent localized sites. Once a molecule occupies a site, no further adsorption can take place. This is described as homogeneous adsorption with uniform energies of ion exchange as all sites possess equal affinity for the adsorbate.

An essential characteristic of Langmuir isotherm can be expressed by a dimensionless constant called equilibrium parameter or separation factor (R_L) [64] which is used to describe the favorability of the adsorption process on the surface of the different types of the clay. The Langmuir separation factor can be represented by the following equation:

$$R_L = \frac{1}{1 + K_L C_o}$$

where K_L is the Langmuir equilibrium constant and C_o is the initial Pb^{2+} ions concentration (mg/L). The value of R_L indicates the type of the isotherm to be either unfavorable ($R_L > 1$), linear ($R_L = 1$), favorable ($0 < R_L < 1$) or irreversible ($R_L = 0$) [65-67]. The more favorable adsorption is reflected by lower R_L values. The R_L values for the adsorption of the Pb^{2+} ions are given in Table 4, which reveals that the values fall in the preferred region (i.e., $0 < R_L < 1$).

The lower values of R_L for RC adsorption (approaching 0) point toward irreversible nature of the adsorption. It can be noted in Table 3 that the R_L values decrease with the increase in the initial Pb^{2+} concentration indicating that the ion exchange is more favorable at higher initial concentration. The favorability of PCN to follow Langmuir model is found to be higher as confirmed by the high square regression (R^2) value (0.9996) than in the case of RC and AAC (0.9938 and 0.9903) respectively, Table 3.

RC		AAC		PCN	
C_o (mg/L)	$R_{L\ Value}$	C_o (mg/L)	$R_{L\ Value}$	C_o (mg/L)	$R_{L\ Value}$
100	-0.0022	42.86	0.038	100	0.0343
120	-0.0018	57.14	0.0287	200	0.0175
140	-0.0016	71.43	0.0231	300	0.0117
180	-0.0012	85.71	0.0193	400	0.0088
220	-0.001	100	0.0166	500	0.007
260	-0.0008	114.29	0.0146	600	0.0059
300	-0.0007	128.57	0.013	700	0.005

Table 3. The R_L values based on the Langmuir isotherm

Fig.9. Freundlich isotherm model for the adsorption process

model for the adsorption of Pb^{2+} ions at different initial concentrations

The Freundlich isotherm [68] is a semi-empirical equation based on the adsorption occurred on heterogeneous surfaces having unequally available sites with different energy of adsorption as well as multilayer sorption. It can be represented by the following form:

$q_e = k_F C_e^{1/n_F}$ which can be expressed in a linear form as $\ln q_e = \ln k_F + \frac{1}{n_F} \ln C_e$

where q_e is the adsorption capacity at equilibrium (mg/g), C_e is the equilibrium concentration of Pb^{2+} ions (mg/L), k_F and n_F are Freundlich isotherm constants related to adsorption capacity and adsorption intensity ((mg/g) (L/mg)$^{1/n}$ and g/L), respectively. This isotherm gives an expression encompassing the surface heterogeneity and the exponential distribution of active sites and their energies. Values of n_F between 2 and 10 show good adsorption [69, 70]. Also from Table 3, the values of n_F were determined to be 5.83 and 3.05 for AAC and PCN, respectively; lying in the range of 1–10, thus is classified as favorable adsorption. The slope ($1/n_F$) range of 0–1 is known to be a measure of adsorption intensity or surface heterogeneity, becoming more heterogeneous as its value gets closer to zero. Whereas, a value below unity implies chemisorption processes where $1/n_F$ above one is an indicative of cooperative adsorption [71].

As assumption of Freundlich isotherm model, the adsorption process on RC was mostly heterogeneous and chemisorption mechanism with $1/n_F$ 0.039. A $1/n_F$ value below unity (0.172 and 0.328 for AAC and PCN, respectively) is indicative of
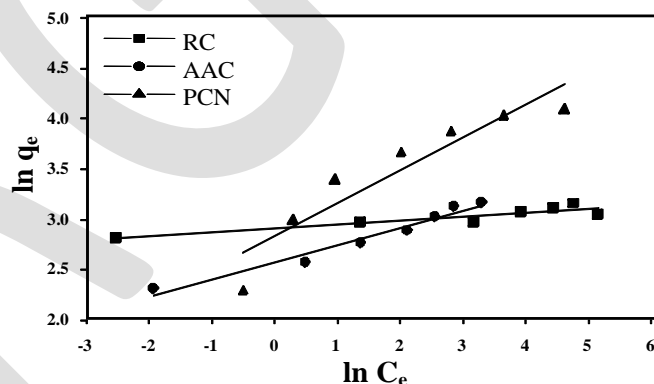
chemisorption process. For PCN, the higher value of the constant k_F 16.947 indicates the higher affinity for Pb^{2+} ions in comparison to AAC 13.007. As shown in figure (9), a plot of $\ln q_e$ versus $\ln C_e$, the best fitting to Freundlich isotherm model is AAC with square regression value (R^2) 0.9661.

Based on energy of activation, we can predict whether an adsorption is physisorption or chemisorption. If the energy of activation is < 8 KJ/mol, the adsorption is physisorption and if the energy of activation is 8-16 KJ/mol, the adsorption is chemisorptions in nature. From Table 3, the adsorption process is physisorption for AAC and PCN where the energy of activation is 4.469 and 1.337 KJ/mol, respectively.

Temperature study

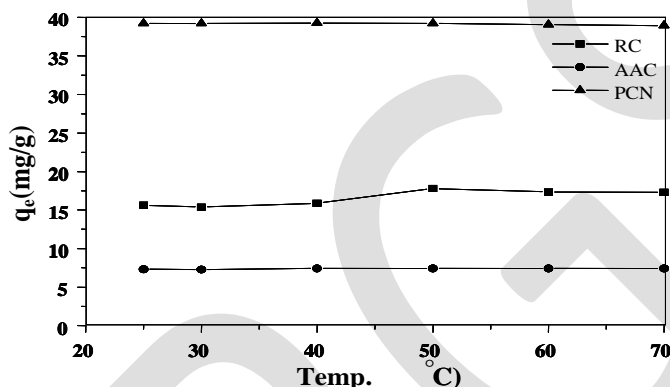## Effect of temperature on the adsorption process

Fig.10. Effect of the temperature on the adsorption of Pb^{2+} ions.

As shown in figure (10), the change in adsorption capacity has the same behavior for RC and its activated form. The graph begins with slight increase in the removal efficiency till reaches its maximum at 50 and 60 ^{o}C, respectively; after which a decrease in the removal process takes place. Using RC, the adsorption capacity begins from 15.39 mg/g till reaches its maximum of 17.79 mg/g at 50 ^{o}C. Beyond 50 ^{o}C slight decrease in the adsorption process occurs. As for AAC, the adsorption capacity begins from 7.3 mg/g till reaches its maximum of 7.44 mg/g at 60 ^{o}C. After 6o ^{o}C slight decrease in the adsorption process takes place. As listed in Table 4, the enthalpy of the adsorption process for RC and its activated form was positive value that means the reaction occurs endothermic. However, when the adsorption occurs as an endothermic process, the increasing temperature favors the adsorption of the adsorbate. Therefore, such an outcome confirms that the best adsorption is obtained with the temperature increase. The previous behavior can be attributed to the fact that, when the temperature increases, the Pb^{2+} ions move more vigorously. As a result, the ions interact more easily with the active sites of the adsorbent surface and result in greater retention. Furthermore, some of the adsorption stages that are originally slow are accelerated by the increase of the activation energy of the system. The slight decrease at the end of each graph can be attributed to the breaking down of the physical adsorption bonds due to the large increase in temperature. The adsorption capacity for PCN begins from 39.22 mg/g with no more increase by increasing the temperature till reaches 50 ^{o}C. After 50 ^{o}C sharp decrease in the adsorption process takes place till it reaches 38.92 mg/g. This behavior may be attributed to the leakage of the physical adsorption bonds due to the increase in the temperature. Also, as listed in Table 4, the enthalpy was negative that means the reaction occurs exothermic. In such process, the adsorption decreases with the increase of the temperature, favoring the adsorbate desorption.

Thermodynamics parameters

The thermodynamic parameters change in Gibb's free energy (ΔG^o), change in enthalpy ΔH^o, and change in entropy ΔS^o for the adsorption of Pb^{2+} ions on each type of clay has been determined by using the following equations:

$$\Delta G^o = \Delta H^o - T\Delta S^o \text{ and } \Delta G^o = -RT \ln K_D \qquad \text{where } K_D = q_e/C_e$$

The relationship between the distribution coefficient and temperature under the assumption that ΔH^o is constant [72] can be expressed by: $\qquad \ln K_D = -\Delta H^o/RT + \Delta S^o/R$

where K_D is the distribution coefficient of the adsorbate, C_e and q_e are the concentrations of Pb^{2+} ions at equilibrium (mg/L) and the adsorption capacity at equilibrium (mg/g), respectively; R is the universal gas constant (8.314 J/mol K) and T is the temperature (K). ΔH^o and ΔS^o parameters can be calculated from the slope and intercept of the plot of $\ln K_D$ vs. 1/T figure (11). ΔG^o was calculated

using the upper equations and all results are listed in Table 5. The spontaneity of the adsorption reactions on the surface of each type of clay was confirmed by the negative value of ΔG°. The positive value of enthalpy indicated that the adsorption process was endothermic for RC and AAC 8.8439 and 7.1522 kJ/mole, respectively. For PCN, the adsorption process seems to be exothermic in nature that explains the decreasing in the adsorption capacity by increasing the temperature. Moreover, the positive value of ΔS° indicates that the degrees of freedom increased at the solid–liquid interface during the adsorption.

Thermodynamic parameters	RC	AAC	PCN
ΔH° (kJ/mol)	8.8439	7.1522	-5.9058
ΔS° (J/mol K)	77.832	90.523	51.574
ΔG° (kJ/mol)	-14.350	-19.823	-21.275

Table 4. Thermodynamic parameters for the adsorption

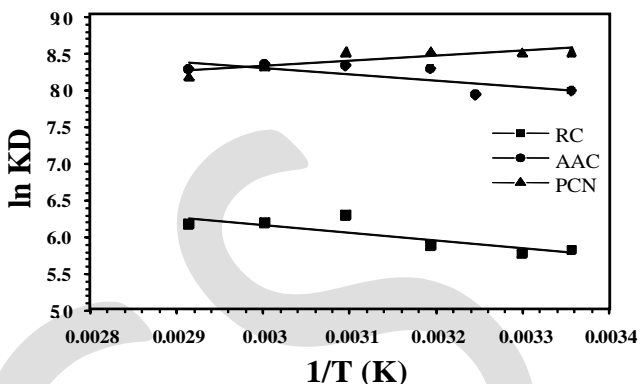of Pb^{2+} ions onto RC, AAC and PCN

Fig.11. Plot of ln K_D Vs. 1/T for the thermodynamics parameters

Effect of the pH on the adsorption process

As shown in figure (12), a gradual increase in the adsorption process in the case of RC from 10.14 mg/g at pH 2 to reach the maximum removal of 22.96 mg/g at pH 5.3, takes place. The adsorption capacity was dropped to 20.37 mg/g at pH 6 and finally total removal of the metal ion at pH 7 is achieved, this is owing to the complete precipitation of the metal ion in the form of hydroxide. In the case of AAC the removal capacity was very low. It begins from 7.39 mg/g at pH 2 with no sharp increase by increasing the pH where it reaches its maximum removal of 7.42 mg/g at pH 6. Finally total removal of the metal ion at pH 7 takes place similarly. For PCN, the removal efficiency was very high. It begins with adsorption capacity of 38.87 mg/g at pH 2 without sharp increase on increasing the pH until maximum removal of 39.28 mg/g at pH 4, then no more increase in the removal of the metal ion till pH 7 where complete precipitation of the metal ion occurred in the form of hydroxide. The low adsorption at low pH was attributed to electrostatic repulsion of both positively charged adsorbent and adsorbate. On the other hand, the H^+ ions present at higher concentration in the aqueous medium compete with the positively charged Pb^{2+} ions for the surface adsorbing sites resulting in a decrease in the removal of Pb^{2+} ions [37, 69].
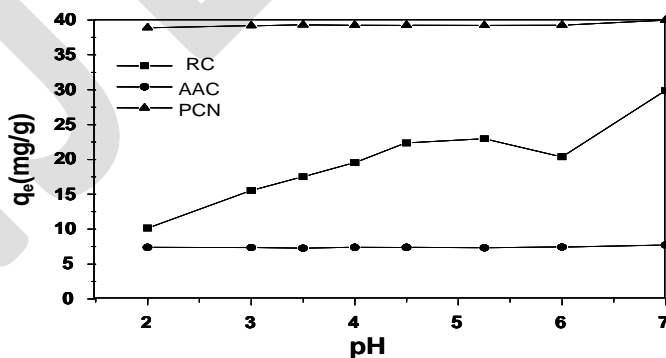

Fig.12. Effect of the pH on the adsorption of Pb^{2+} ions.

Real sample treatment

Real surface water samples taken directly from the River Nile are collected from different places in Beni-Suef governorate in order to study the matrix effect on the adsorption process. The samples are spiked with lead ions and the batch adsorption method was applied.

The removal efficiency was found to be 57.58%, 81.88% and 98.25% for RC, AAC and PCN, respectively; proving that PCN, as expected, has the best removal efficiency. The equilibrium adsorption capacity for PCN is nearly twice that for RC. The equilibrium adsorption capacity values for the three adsorbents are illustrated in table 5

Table 5. Analysis of real samples:

Surface water analysis	$C_o = 100$ (mg/L)				$C_o = 200$ (mg/L)			
	C_e (mg/L)	Removal amount (mg/L)	Removal percent (%)	q_e (mg/g)	C_e (mg/L)	Removal amount (mg/L)	Removal percent (%)	q_e (mg/g)
RC	3.55	96.45	96.45	19.29	84.84	115.16	57.58	23.03
AAC	12.68	87.32	87.32	17.46	36.25	163.75	81.88	32.75
PCN	0.28	99.72	99.72	19.95	3.5	196.5	98.25	39.3

CONCLUSION

Natural raw montmorillonite clay mineral RC, its sulfuric acid activated form AAC and its polymer/clay nanocomposite PCN were applied for the removal of Pb^{2+} from authentic samples and spiked real surface water samples collected directly from the River Nile. TGA, XRD, IR and SEM analyses were used to characterize the mineralogical compositions of RC, AAC and functionalized PCN. Batch adsorption method was applied and optimum conditions for adsorption (adsorbent dosage, contact time, effect of temperature, effect of pH and initial lead concentration) were evaluated. Langmuir (L), Freundlich (F), isotherm equations have been applied to analyze the obtained experimental data. The maximum adsorption capacity for RC, AAC and PCN was found to be 21.73, 24.52 and 61.82 mg/g with respect to Langmuir.

REFERENCES:

[1] N. Burham, A. Mamdouh, M.F.El-Shahat, Separation and Determination of Cd^{2+}, Pb^{2+} and Cu^{2+} from Water Samples Using Chemically Modified Groundnut Shells, International Journal of Advanced Research 2 (1) (2014) 755-765.

[2] M. Hua, S. Zhang, B. Pan, W. Zhang, L. Lv, Q. Zhang, Heavy metal removal from water/wastewater by nanosized metal oxides, Journal of Hazardous Materials 211– 212 (2012) 317– 331.

[3] A. Singh, R.K. Sharma, M. Agrawal, F.M. Marshall, Health risk assessment of heavy metals via dietary intake of foodstuffs from the wastewater irrigated site of a dry tropical area of India, Food Chem. Toxicol. 48 (2010) 611–619.

[4] M. Jamil, M.S. Zia, M. Qasim, Contamination of agro-ecosystem and human health hazards from wastewater used for irrigation, J. Chem. Soc. Pak. 32 (2010) 370–378.

[5] S. Khan, Q. Cao, Y.M. Zheng, Y.Z. Huang, Y.G. Zhu, Health risks of heavy metals in contaminated soils and food crops irrigated with wastewater in Beijing, China, Environ. Pollut. 152 (2008) 686–692.

[6] S.H. Peng, W.X. Wang, X.D. Li, Y.F. Yen, Metal partitioning in river sediments measured by sequential extraction and biomimetic approaches, Chemosphere 57 (2004) 839–851.

[7] X. Lu, L. Wang, L. Li, Y.K. Lei, L. Huang, D. Kang, Multivariate statistical analysis of heavy metals in street dust of Baoji, NW China, Journal of Hazardous Materials 173 (7) (2010) 744–749.

[8] A.D.K. Banerjee, Heavy metal levels and solid phase speciation in street dusts of Delhi, India, Environmental Pollution 123 (1) (2003) 95–105.

[9] S. Charlesworth, M. Everett, R. McCarthy, A. Ordóñez, E. de Miguel, A comparative study of heavy metal concentration and distribution in deposited street dusts in a large and a small urban area: Birmingham and Coventry, West Midlands, UK, Environment International 29 (5) (2003) 563-573.

[10] H.T. Fan, J.B. Wu, X.L. Fan, D.S. Zhang, Z.J. Su, F. Yan, T. Sun, Removal of cadmium(II) and lead(II) from aqueous solution using sulfur-functionalized silica prepared by hydrothermal-assisted grafting method, Chemical Engineering Journal 198/199 (198) (2012) 355–360.

[11] Global health risks: Mortality and burden of disease attributable to selected major risks, Geneva, World Health Organization, 2009, (http://www.who.int/healthinfo/global_burden_disease/ GlobalHealthRisks_report_full.pdf).

[12] Lead in Drinking-water: Background document for development of WHO Guidelines for Drinking-water Quality, 20 Avenue Appia, 1211 Geneva 27, World Health Organization, 2011, (http://www.who.int/ipcs/assessment/public_health/lead_other/en/).

[13] Exposure to lead: A major public health concern, Geneva, World Health Organization, 2010, (http://www.who.int/ipcs/features/lead..pdf).

[14] J.T. Nwabanne, P.K. Igbokwe, Adsorption performance of packed bed column for the removal of lead(II) using oil palm fibre, Int. J. Appl. Sci. Technol. 2 (5)(2012) 106–115.

[15] S. Ong, C. Seng, P. Lim, Kinetics of adsorption of Cu (II) and Cd (II) from aqueous solution on husk and modified rice husk, EJEAFche 6 (2) (2007) 1764-1774.

[16] S. Qaiser, A.R. Saleem, M.M. Ahmed, Heavy metal uptake by agro based waste materials, Environmental Biotechnol. 10(3) (2007) 1-8.

[17] Brief guide to analytical methods for measuring lead in blood, Geneva, World Health Organization 2011, (http://apps.who.int/iris/bitstream/10665/77912/1/9789241502139_eng.pdf?ua=1).

[18] H.Z. Mousavi, A. Hosseynifar, V. Jahed, S.A.M. Dehghani, Removal of lead from aqueous solution using waste tire rubber ash as an adsorbent, Braz. J. Chem. Eng. 27 (1) (2010) 79-87.

[19] S.Tong, Y.E.V. Schirnding, T. Prapamontol, Environmental lead exposure: a public health problem of global dimensions, Bulletin of the World Health Organization 78 (9) (2000) 1068-1077.

[20] Y.Y. Long, Y.J. Feng, S.S. Cai, L.F. Hu, D.S. Shen, Reduction of heavy metals in residues from the dismantling of waste electrical and electronic equipment before incineration, Journal of Hazardous Materials 272 (2014) 59–65.

[21] M. Bilal, J.A. Shah, T. Ashfaq, S.M.H. Gardazi, A.A. Tahir, A. Pervez, H. Haroon, Q. Mahmood, Waste biomass adsorbents for copper removal from industrial wastewater: A review, Journal of Hazardous Materials 263 (2013) 322– 333.

[22] N. Li, L. Zhang, Y. Chen, M. Fang, H. Wang, Highly efficient, irreversible and selective ion exchange property of layered titanate nanostructures, Adv. Funct. Mater. 22 (2012) 835-841.

[23] K. Dermentzis, Removal of nickel from electroplating rinse waters using electrostatic shielding electrodialysis/electrodeionization, Journal of Hazardous Materials 173 (2010) 647-652.

[24] P. Grimshaw, J.M. Calo, G. Hradil, Cyclic electrowinning/precipitation (CEP) system for the removal of heavy metal mixtures from aqueous solutions, Chemical Engineering Journal 175 (2011) 103- 109.

[25] K. Mansouri, A. Hannachi, A. Abdel-Wahab, N. Bensalah, Electrochemically dissolved aluminum coagulants for the removal of natural organic matter from synthetic and real industrial wastewaters, Ind. Eng. Chem. Res. 51 (2012) 2428-2437.

[26] S. Malamis, E. Katsou, K. Takopoulos, P. Demetriou, M. Loizidou, Assessment of metal removal, biomass activity and RO concentrate treatment in an MBR-RO system, Journal of Hazardous Materials 209-210 (2012) 1-8.

[27] A.Y. Dursun, A comparative study on determination of the equilibrium, kinetic and thermodynamic parameters of biosorption of copper (II) and lead (II) ions onto pretreated Aspergillus niger, Biochemical Engineering Journal 28 (2006) 187–195.

[28] L. Deng, X. Zhu, X. Wang, Y. Su, H. Su, Biosorption of copper(II) from aqueous solutions by green alga Cladophora fascicularis, Biodegradation 18 (2007) 393–402.

[29] M.A. Hanif, R. Nadeem, H.N. Bhatti, N.R. Ahmad, T.M. Ansari, Ni(II) biosorption by Cassia fistula (Golden Shower) biomass, Journal of Hazardous Materials 139 (2007) 345–355.

[30] B. Preetha, T. Viruthagiri, Batch and continuous biosorption of chromium (VI) by Rhizopus arrhizus, Separation and Purification Technology 57 (2007) 126–133.

[31] D. Satapathy, G.S. Natarajan, Potassium bromate modification of the granular activated carbon and its effect on nickel adsorption, Adsorption 12 (2006) 147–154.

[32] K. Vijayaraghavan, K. Palanivelu, M. Velan, Biosorption of copper(II) and cobalt(II) from aqueous solutions by crab shell particles, Bioresource Technology 97 (2006) 1411–1419.

[33] X. Wang, S. Xia, L. Chen, J. Zhao, J. Chovelon, J. Nicole, Biosorption of cadmium(I1) and lead(I1) ions from aqueous solutions onto dried activated sludge, Journal of Environmental Sciences 18 (2006) 840–844.

[34] B.J. Pan, B.C. Pan, W.M. Zhang, L. Lv, Q.X. Zhang, S.R. Zheng, Development of polymeric and polymer-based hybrid adsorbents for pollutants removal from waters, Chemical Engineering Journal 151 (2009) 19–29.

[35] C.O. Ijagbemi, M.H. Baek, D.S. Kim, Adsorptive performance of un-calcined sodium exchanged and acid modified montmorillonite for Ni^{2+} removal: Equilibrium, kinetics, thermodynamics and regeneration studies, Journal of Hazardous Materials 174 (2010) 746–755.

[36] M. Erdem, A. Özverdi, Lead adsorption from aqueous solution on to siderite, Sep. Purif. Technol. 42(3) (2005) 259–264.

[37] R. Petrus, J.K. Warcho, Heavy metal removal by clinoptilolite: An equilibrium study in multi-component systems, Water Research 39 (2005) 819–830.

[38] S. Çoruh, The removal of zinc ions by natural and conditioned clinoptilolites, Desalination 225 (2008) 41–57.

[39] Chaari, E. Fakhfakh, S. Chakroun, J. Bouzid, N. Boujelben, M. Feki, F. Rocha, F. Jamoussi, Lead removal from aqueous solutions by a Tunisian smectitic clay, Journal of Hazardous Materials 156 (2008) 545–551.

[40] R. Naseem, S.S. Tahir, Removal of Pb(II) from aqueous/acidic solutions by using bentonite as an adsorbent. Water Res., 35(16) (2001) 3982–3986.

[41] J. Peric, M. Trogo, M.N. Vukojevic, Removal of zinc, copper and lead by natural zeolite: a comparison of adsorption isotherms, Water Res., 38 (2004) 1893–1899.

[42] S. Babel, T.A. Kurniawan, Low-cost adsorbents for heavy metals uptake from contaminated water: review, Journal of Hazardous Materials, 97 (2003) 291–243.

[43] T.G. Merlain, N.J. Nsami, K.J. Mbadcam, Adsorption of Copper (II) Ions from Aqueous Solution onto Synthetic Goethite and Two Naturally Available Red Soils from Yaoundé-Cameroon, British Biotechnology Journal 3(3) (2013) 221-235.

[44] Y. Yu, J.G. Shapter, R.P. Filcoff, J.W. Bennett, A.V. Ellis, Copper removal using bio-inspired polydopamine coated natural zeolites, Journal of Hazardous Materials 273 (2014) 174–182.

[45] D. Chen, L. Cao, T.L. Hanley, R.A. Caruso, Facile synthesis of monodisperse zirconium titanium oxide microspheres with varying compositions and high surface areas for heavy metal ion sequestration, Adv. Funct. Mater. 22 (2012) 1966-1971.

[46] K.H. Chu, Removal of copper from aqueous solution by chitosan in prawn shell: adsorption equilibrium and kinetics, Journal of Hazardous Materials 90 (2002) 77–95.

[47] N.N. Maximous, G.F. Nakhla, W.K. Wan, Removal of Heavy Metals from Wastewater by Adsorption and Membrane Processes: a Comparative Study, World Academy of Science, Engineering and Technology, 40 (2010) 520-531.

[48] P. Kar, N.C. Pradhan, B. Adhikari, A novel route for the synthesis of processable conducting poly (m-aminophenol), Mat. Chem. Phys 111 (2008) 59–64.

[49] S.M. Sayyah, A.A. Bahgat, H.M.A. El-Salam, Kinetic studies of the aqueous oxidative polymerization of 3-hydroxyaniline and characterization of the polymer obtained, Int. J. Polym. Mater. 51 (2002) 291–314.

[50] F.A. Rafiqi, M.S. Rather, K. Majid, Doping polyaniline with copper bisglycinate[Cu(gly)2]: Synthesis, characterization and thermal study, Synthetic Metals 171 (2013) 32– 38.

[51] B.L. Rivas, C.O. Sanchez, J.C. Bernede, P. Mollinie, Synthesis, characterization, and properties of poly(2- and 3-aminophenol) and poly(2- and 3-aminophenol)-Cu(II) materials, Polym. Bull. 49 (2002) 257–264.

[52] M.T. Angaji1, A.Z. Zinali, N.T. Qazvini, Study of Physical, Chemical and Morphological Alterations of Smectite Clay upon Activation and Functionalization via the Acid Treatment, World Journal of Nano Science and Engineering 3 (2013) 161-168.

[53] A.R. Kula, H. Koyuncu, Adsorption of Pb(II) ions from aqueous solution by native and activated bentonite: Kinetic, equilibrium and thermodynamic study, Journal of Hazardous Materials 179 (2010) 332–339.

[54] S. Lagergren, About the theory of so called adsorption of soluble substance, Kungliga svenska ertenskapsakademiens, Hand Linger 24 (1898) 1–39.

[55] M.M. Rao, D.K. Ramana, K. Seshaiah, M.C. Wang, S.W.C. Chien, Removal of some metal ions by activated carbon prepared from Phaseolus aureus hulls, Journal of Hazardous Materials 166 (2009) 1006–1013.

[56] Y.S. Ho, G. McKay, Pseudo-second order model for sorption process, Process Biochem. 34 (1999) 451–465.

[57] Y.S. Ho, Selection of optimum sorption isotherm, Carbon 42 (2004) 2115–2116.

[58] Q. Dong, J. Liu, L. Song, G. Shao, Novel zwitterionic inorganic-organic hybrids: synthesis of hybrid adsorbents and their applications for Cu^{2+} removal, Journal of Hazardous Materials 186 (2011) 1335–1342.

[59] W.J. Webber, J.C. Morris, Kinetics of adsorption on carbon from solution, J. Sanit. Eng. Div. Am. Soc. Civil Eng. 89 (1963) 31–60.

[60] I. Langmuir, The constitution and fundamental properties of solids and liquids, J. Am. Chem. Soc. 38 (11) (1916) 2221–2295.

[61]S.Larous, A.-H. Meniai, M.B. Lehocine, Experimental study of the removal of copper from aqueous solutions by adsorption using sawdust, Desalination 185 (2005) 483–490.

[62] S.J. Allen, G. Mckay, J.F. Porter, Adsorption isotherm models for basic dye adsorption by peat in single and binary component systems, J. Colloid Interface Sci. 280 (2004) 322–333.

[63] S. Kundu, A.K. Gupta, Arsenic adsorption onto iron oxide-coated cement (IOCC): regression analysis of equilibrium data with several isotherm models and their optimization, Chemical Engineering Journal 122 (2006) 93–106.

[64] T.W. Webber, R.K. Chakkravorti, Pore and solid diffusion models for fixed-bed adsorbers, AIChE J. 20 (1974) 228–238.

[65] A. Sari, M. Tuzen, D. Citak, M. Soylak, Equilibrium, kinetic and thermodynamic studies of adsorption of Pb(II) from aqueous solution onto Turkish kaolinite clay, Journal of Hazardous Materials 149 (2007) 283–291.

[66] Y.S. Ho, C.T. Huang, H.W. Huang, Equilibrium sorption isotherm for metal ions on tree fern, Process Biochem. 37 (2002) 1421–1430.

[67] M.J. Angove, B.B. Johson, J.D. Wells, Adsorption of cadmium(II) on kaolinite, Colloid Surf. A: Phys. Eng. Aspects 126 (1997) 137–147.

[68] H.M.F. Freundlich, over the adsorption in solution, J. Phys. Chem. 57 (1906) 385–471.

[69] M. Rao, A.G. Bhole, Chromium removal by adsorption using fly ash and bagasse, J. Indian Water Works Assoc. XXXIII (1) (2001) 97–100.

[70] C. Raji, T.S. Anirudhan, Chromium (VI) adsorption by sawdust: kinetics and equilibrium, Indian J. Chem. Technol. 4 (1997) 228–236.

[71] F. Haghseresht, G. Lu, Adsorption characteristics of phenolic compounds onto coal-reject-derived adsorbents, Energy Fuels 12 (1998) 1100–1107.

[72] B.M.W.P.K. Amarasinghe, R.A. Williams, Tea waste as a low cost adsorbent for the removal of Cu and Pb from wastewater, Chemical Engineering Journal 132 (2007) 299–309